Green Chemistry

PAPER

View Article Online
View Journal | View Issue

Cite this: *Green Chem.*, 2022, **24**, 9101

Catalytic production of tetrahydropyran (THP): a biomass-derived, economically competitive solvent with demonstrated use in plastic dissolution†

Raka G. Dastidar,[a] Min Soo Kim,[a] Panzheng Zhou,[a] Zaneta Luo,[a] Changxia Shi,[b] Kevin J. Barnett,[c] Daniel J. McClelland,[c] Eugene Y.-X. Chen,[b] Reid C. Van Lehn[a] and George W. Huber*[a]

Received 14th September 2022,
Accepted 31st October 2022

DOI: 10.1039/d2gc03475a

rsc.li/greenchem

Tetrahydropyran (THP) is a five-carbon heterocyclic ether that is non-carcinogenic, non-peroxide forming, biodegradable, and economically competitive with tetrahydrofuran (THF) as a solvent. In this work, THP has been synthesized from renewable biomass at >99.8% selectivity and 98% yield *via* hydrogenation of furfural-derived 3,4-dihydropyran (DHP) over Ni/SiO_2 in a continuous flow reactor at 150–200 °C. The apparent activation energy of THP formation is 31 kJ mol^{-1}, and the reaction orders with respect to the partial pressures of H_2, DHP, and THP are: 2, 1, and −0.3. The kinetic data has been fitted to a Hougen–Watson model where the rate limiting step is the hydrogenation of adsorbed DHP. Ni/SiO_2 is shown to have a low deactivation rate constant of 0.012 h^{-1} over 100 h time on stream and can be regenerated *in situ*. As a performance advantage, THP is shown to be resistant to ring opening polymerization under strongly acidic conditions that THF is not, revealing it to be a superior solvent. The minimum selling price of THP is competitive with the market price of THF ($900–1400 per ton) at a DHP feedstock cost of $1000 per ton. Conductor-like Screening Model for Real Solvents (COSMO-RS) and molecular dynamics (MD) simulations with 1008 solvents and 8 common plastics have demonstrated that THP can serve as an alternative solvent to THF, 2-methyltetrahydrofuran (MeTHF), and cyclopentyl methyl ether (CPME) for plastic dissolution, especially low-density polyethylene (LDPE), polypropylene (PP), polystyrene (PS) and polyvinyl chloride (PVC). This work establishes THP as a green solvent with excellent thermal, chemical and peroxidative stability that can be used for numerous applications, including waste plastic recycling.

1. Introduction

Catalytic upgrading of lignocellulosic biomass offers a sustainable route to green solvents with superior properties.[1,2] The global solvent market is projected to reach $67 billion in 2028,[3] but most industrial solvents in use today are petroleum-derived.[4] Ethers and aromatic solvents are also extremely hazardous as peroxide formers,[5] carcinogens,[6] reproductive hazards,[7] and/or neurotoxins.[8] While some research has demonstrated the production of ether solvents from biomass, they suffer from peroxide formation[9] and the high price of precious metal catalysts/reactants.[10] In this work, we introduce an approach to produce tetrahydropyran (THP) from biobased furfural. THP is a five-carbon heterocyclic ether that is non-carcinogenic,[11] biodegradable,[12] and non-peroxide forming even after 30 days of exposure to air.[13]

The solvent properties of THP, 2-methyl-THF (MeTHF), tetrahydrofuran (THF), and diethyl ether are shown in Table 1. THP has the highest boiling point (88 °C) among the listed solvents, imparting it with the lowest vapor pressure and excellent thermal stability. Separation and recovery of THP from aqueous reaction mixtures is simpler since it has a lower solubility in water compared to THF (8.57 wt% solubility for THP *vs.* miscibility of THF in water). Moreover, THP has the highest autoxidation stability to peroxide formation.[14] DFT calculations show that this is due to higher energy barriers for both hydrogen abstraction from THP and subsequent molecular oxygen capture by the generated THP radical.[15] The flash

[a]*Department of Chemical and Biological Engineering, University of Wisconsin-Madison, Wisconsin 53706, USA. E-mail: gwhuber@wisc.edu*
[b]*Department of Chemistry, Colorado State University, Fort Collins, Colorado 80523, USA*
[c]*Pyran Inc., 505 South Rosa Road, Suite 112, Madison, Wisconsin 53719, USA*
† Electronic supplementary information (ESI) available. See DOI: https://doi.org/10.1039/d2gc03475a

Table 1 Solvent properties of tetrahydropyran, 2-methyltetrahydrofuran, tetrahydrofuran, and diethyl ether

Solvent property	Tetrahydropyran	2-Methyltetrahydrofuran	Tetrahydrofuran	Diethyl ether
Structure				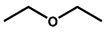
Feedstock	Biomass (3,4-dihydropyran)	Biomass (furfural)	Petroleum (1,4-butanediol)	Petroleum (ethylene)
Molar mass (g mol^{-1})	86.13	86.13	72.10	74.12
Boiling point (°C)	88.0	80.2	66.0	34.6
Melting point (°C)	−45	−136	−108.5	−116.3
Flash point (°C)	−16	−11	−14	−45
Viscosity (cP)	0.79	0.54	0.48	0.28
Density (g cm^{-3})	0.88	0.85	0.88	0.71
Solubility in water (wt%)	8.57	14	Miscible	6.05
Dielectric constant	5.7	6.9	7.6	4.3
Dipole moment (D)	1.6	1.4	1.6	1.1
Surface tension (mN m^{-1})	27.3	25.5	29.5	17
Peroxide formation (ppm at 3 h)[10,21]	None	>30	>100	>200

point, density, dielectric constant, dipole moment, and surface tension of THP are similar to those of MeTHF and THF. Owing to these favorable solvent properties, THP has been used to replace THF as the solvent for radical chain reactions, such as tributylin hydride mediated reduction and cyclization (TTMSS).[13] THP has also been used as the solvent for anionic polymerization of styrene,[16] and α-methylstyrene.[17] Another application of THP is in the form of organic electrolytes like lithium imide/THP for 4 V lithium metal rechargeable batteries.[18] Compared to other cyclic ether solvents, THP exhibited >95% Li cycling efficiency, >300 cycle life, and highest cathodic and anodic stability at high temperatures. Methyl THP has been successfully used as the solvent for organic reactions including radical, Grignard, Wittig, and organometallic reactions.[19] In the pharmaceuticals industry, substituted THP compounds are used for their analgesic, anti-inflammatory, and cytotoxic activities.[20]

THP has been synthesized by dehydration of 1,5-pentanediol (1,5-PDO) over ZrO_2–ZnO but the selectivity is poor (54%).[22] The market price of petroleum-based 1,5-PDO is also high (>$5000 per ton) since it is formed in low quantities as a byproduct of petroleum-based KA oil oxidation.[23] Unlike petroleum, lignocellulosic biomass is rich in five-carbon feedstock in the form of xylose – the second most abundant sugar in the world.[24] Xylose is dehydrated to produce furfural, which is a major commodity chemical with a projected market volume of 400 000 tons by 2024.[25] Tetrahydrofurfuryl alcohol (THFA) is then synthesized in near quantitative yields from hydrogenation of furfural over Ni/SiO_2.[26] The patented "PyranDiol" technology that we developed is used to produce 3,4-dihydropyran (DHP) from dehydration of THFA over γ-Al_2O_3 at 375 °C, followed by hydration and hydrogenation reactions to produce 1,5-PDO.[27–29] In this work, THP production has been demonstrated from hydrogenation of DHP over Ni/SiO_2, as shown in Scheme 1. The intrinsic kinetics of this reaction have been identified, including apparent activation energies and reaction orders, and a Hougen–Watson kinetic model has been developed. The minimum selling price of THP and its variation with production volume and DHP feedstock price have been determined. Lastly, the use of THP as a solvent has been demonstrated using a combination of computational and experimental approaches. We hope to convince the readers that THP can become a low-cost biomass based renewable solvent in several promising applications.

2. Experimental section

2.1. Catalytic experiments

DHP hydrogenation to THP was carried out in a down-flow packed bed reactor. Ni/SiO_2 (0.1 g) was loaded into a stainless-steel reactor tube (316 SS, 15″ length, 1/4″ OD) and held in place by packing quartz wool and glass beads on both ends. The reactor tube was enclosed in an aluminum heating block with an embedded thermocouple and placed in a clamshell furnace (Thermo Scientific Lindberg Blue M). System pressure was maintained at 200 psig using a dome-loaded back pressure regulator (Equilibar) with Argon (Airgas, UHP grade) as the

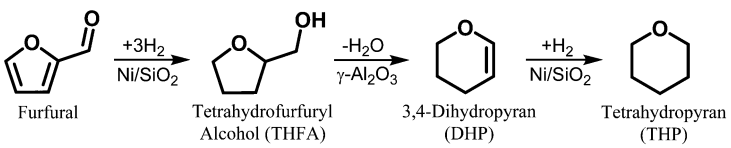

Scheme 1 Reaction pathway for THP production from hydrogenation of furfural-derived DHP.

pilot fluid. At the start of each experiment, Ni/SiO_2 was reduced *in situ* with 100 mL min^{-1} of H_2 (Airgas, UHP grade) at 500 °C with 100 °C h^{-1} ramp and 5 h hold. The furnace temperature was then reduced to 150 °C and the feed, DHP (99%, Acros Organics), was pumped in at 0.1 mL min^{-1} using an HPLC pump (Eldex). H_2 co-feed was maintained at 100 mL min^{-1} for the duration of the reaction. For partial pressure experiments with THP co-feed, THP was purchased from Sigma-Aldrich (anhydrous, 99%). The products were collected in a stainless-steel vessel chilled with a circulating water/ethylene glycol solution maintained at −20 °C to prevent losses to the gas phase. The reaction time on stream was measured from the time it took the reactor to reach the target temperature and pressure. Product samples were drawn every 3–6 hours, and the total reaction time was 24 h. The products were identified by gas chromatography-mass spectrometry (GC-MS) with a Shimadzu GCMS-QP2010 equipped with an RTX-VMS column and quadrupole MS and quantified using a Shimadzu GC 2010 with a flame ionization detector (GC-FID). The equations used to calculate the product yield, selectivity, flow rates, and ^{13}C area enhancements are defined in eqn (1) and (2).

$$\text{Product rate} = \text{mmol}_{\text{product}}\ \text{h}^{-1}\ \text{g}_{\text{catalyst}}{}^{-1} \quad (1)$$

$$\text{Product selectivity} = \text{mmol}_{\text{product}}\ \text{mmol}_{\text{total product}}{}^{-1} \quad (2)$$

2.2. Catalyst preparation and characterization

SiO_2 was purchased from Sigma-Aldrich and dried overnight in an air oven at 110 °C. Ni/SiO_2 catalysts containing 10 wt% Ni (labeled 10-Ni/SiO_2) were synthesized using incipient wetness impregnation of an aqueous solution of $Ni(NO_3)_2{\cdot}6H_2O$ (Sigma-Aldrich) onto SiO_2. Ni/SiO_2 catalysts containing 30 wt% Ni (labeled 30-Ni/SiO_2) were purchased from Clariant. All catalysts were dried overnight in an air oven again at 110 °C, then calcined in a muffle furnace at 500 °C for 10 h in an air atmosphere. Temperature-programmed reduction (TPR) and CO chemisorption of the catalyst were carried out using a Micrometrics AutoChem II 2920 instrument equipped with an MKS Cirrus 2 quadrupole mass spectrometer. For the TPR, 100 mg of catalyst was loaded into a quartz tube and heated from 50 to 900 °C at 10 °C min^{-1} in 25 mL min^{-1} flow of 10% H_2/Ar. Fig. S1† shows the temperature-programmed reduction (TPR) profile of 10-Ni/SiO_2. For CO chemisorption, 100 mg of catalyst was first reduced at 500 °C for 4 h with a 10 °C min^{-1} ramp in 10% H_2/Ar, then cooled to 50 °C in He, followed by CO pulsing in 0.5 mL pulses. The surface Ni sites were measured assuming a stoichiometric factor of 1, *i.e.* one CO molecule chemisorbed on one Ni surface atom.

N_2 physisorption of the catalyst was carried out using a Micromeritics ASAP 2020 instrument. Nickel content of the catalyst was measured using inductively coupled plasma – optical emission spectroscopy (ICP-OES) using a VISTA-MPX instrument. Thermogravimetric analysis (TGA) of the spent catalyst was carried out in a TA Instruments TGA Q500 V6 instrument. 10 mg of the catalyst was placed into a platinum pan, inserted into the instrument, then analyzed with 50 mL min^{-1} of the sample gas (N_2 or O_2) while heating from 25 to 600 °C at 10 °C min^{-1}.

2.3. Polymerization experiments

Polymerizations were performed in glass reactors inside an inert glovebox or on a Schlenk line. The monomer (THF or THP, or a 1 : 1 mixture of THF and THP) and catalyst ($BF_3{\cdot}Et_2O$, CF_3SO_3H or $Yb(OTf)_3$) were added into the reactor. For the polymerization at −30 °C, the reactor was placed in the glovebox freezer; for the polymerization at 0 °C, the reactor was taken out of the glovebox and placed in a freezer with the temperature of 0 °C; for the polymerization at 80 °C, the reactor was taken out of the glovebox and placed in an oil bath with the temperature of 80 °C. After a desired time, the polymerization was quenched by NaOH aqueous solution. The quenched mixture was then precipitated into cold methanol to remove the catalyst residue, and the obtained polymer was dried in a vacuum oven at room temperature overnight to a constant weight. The following polymer properties were determined: melting transition (T_m) temperature, glass transition (T_g) temperature, decomposition (T_d) temperature, weight-average molecular weight (M_w), number-average molecular weight (M_n), and dispersity index ($Đ = M_w/M_n$). The experimental details of polymer characterization have been summarized in the ESI.†

2.4. Techno-economic analysis

The minimum selling price (MSP) of THP was estimated by a techno-economic analysis (TEA) to determine the economic feasibility of the THP production process. The THP production simulation model was developed in Aspen Plus (V12.0 Aspen Technology) based on the experimental data reported here. Equipment sizing and cost analysis for the corresponding equipment were estimated using Aspen Process Economic Analyzer (V12.0 Aspen Technology). Fig. 1 shows the process flow diagram for THP production from hydrogenation of DHP with 30-Ni/SiO_2 at 200 °C. Table S1† lists the temperature, pressure, and mass flow rate of each stream. DHP is pumped into the system *via* Stream 1 and heated up to 200 °C. The H_2/DHP molar ratio in the inlet stream (Stream 2) to the catalytic reactor (R-1) is maintained at 34. The product stream from R-1 (Stream 3) is cooled from 200 °C to 25 °C, and then sent to the fractionating column (F-1). High purity product THP is collected from the bottom while unreacted H_2 and small amounts of DHP are removed from the top (Stream 4). 3% of Stream 4 is purged, and the rest is recycled back to R-1. The H_2 makeup stream (Stream 6) is used to maintain a constant H_2/DHP molar ratio of 34 in R-1. The lifetime of the catalyst is assumed to be three months on stream. After three months, the reaction is stopped and the catalyst is regenerated, while the DHP is fed into a parallel reactor.

2.5. Computational modeling of solvent properties

To investigate the potential applications of THP as a solvent, we employed a set of computational tools to identify similar

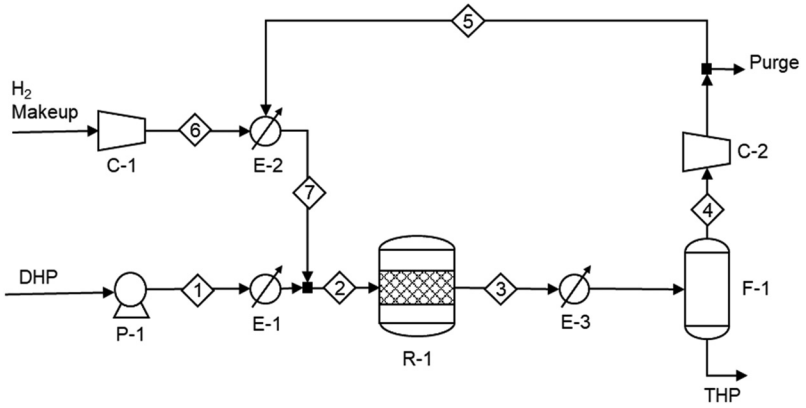

Fig. 1 Process flow diagram for THP production from hydrogenation of DHP in a packed bed reactor. C: compressor, E: heat exchanger, F: flash column, P: pump, R: reactor.

solvents to THP and study the potential use of THP for polymer dissolution. These computational methods include the Conductor-like Screening Model for Real Solvents (COSMO-RS)[30,31] and classical molecular dynamics (MD) simulations. COSMO-RS can predict the thermodynamic properties of multicomponent systems based on quantum mechanical calculations and statistical thermodynamics methods.[32] It represents each chemical compound by the probability distribution profile of the screening charge densities on the molecular surface, which is called the σ-profile. We quantified solvent similarity by calculating the Euclidean distance between the σ-profiles of two solvents. COSMO-RS solubility predictions were performed using the COSMOtherm 19 software with the BP_TZVP_19 parameterization and pre-calculated COSMO files from the database COSMObase-1901-BP-TZVP.[33,34] Fig. 2 shows some examples of screening charge distributions of THP, THF, and a low density polyethylene (LDPE) oligomer. In previous work, we employed these tools to predict the solubility of 8 common polymers in 1007 solvents at multiple temperatures.[35,36] This information was used to populate the polymer solubility database and to predict polymer solubility in THP and other solvents in this work. Further MD simulations of oligomer molecules in different solvents were performed to support the dissolution predictions. The details of the MD simulation setup have been summarized in the ESI.†

3. Results and discussion

3.1. DHP hydrogenation to THP over Ni/SiO_2

The thermodynamics of DHP hydrogenation to THP were evaluated using Aspen Plus prior to kinetic experiments. Since the over-hydrogenolysis of THP produces 1-pentanol as the side product, calculations for THP hydrogenation to 1-pentanol were also evaluated.[37] Fig. 3 shows the variation in ΔG_{rxn} and ΔH_{rxn} from 100–500 °C at 200 psig. The ΔG_{rxn} of DHP hydrogenation to THP decreases in magnitude from −55 kJ mol^{-1} at

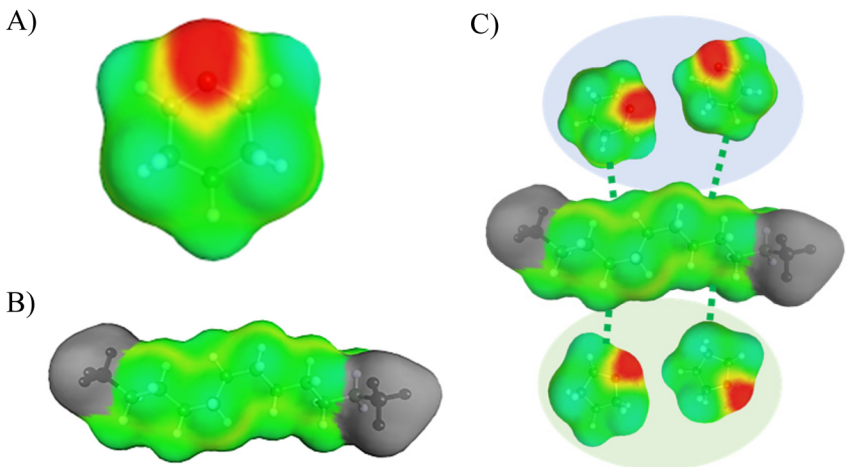

Fig. 2 Screening charge distributions from COSMO-RS for: (A) THP; (B) LDPE oligomer; (C) intermolecular interactions of an LDPE oligomer with THP (top), and THF (bottom).

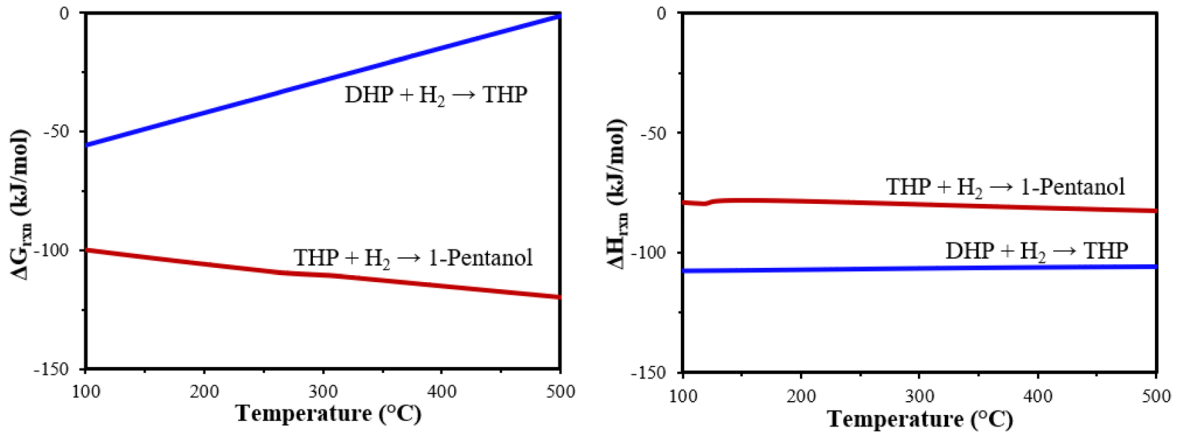

Fig. 3 ΔG_{rxn} and ΔH_{rxn} for DHP hydrogenation to THP and over-hydrogenolysis of THP to 1-pentanol, as calculated from Aspen Plus. Simulation conditions: 200 psig, Peng–Robinson package.

100 °C to −1.4 kJ mol^{-1} at 500 °C. THP hydrogenation to 1-pentanol is increasingly exergonic with rising temperatures, with the ΔG_{rxn} increasing from −100 kJ mol^{-1} at 100 °C to −120 kJ mol^{-1} at 500 °C. Both reactions are exothermic over the entire range of temperatures simulated. The ΔH_{rxn} of DHP hydrogenation to THP is −105 kJ mol^{-1}, while the ΔH_{rxn} of THP hydrogenation to 1-pentanol is less exothermic at −80 kJ mol^{-1} over the full temperature range. These calculations demonstrate that 1-pentanol is the thermodynamically favored product, especially at higher temperatures. The subsequent kinetic studies were conducted at lower temperatures between 150–200 °C.

The kinetics of THP formation was studied using a continuous flow reactor packed with Ni/SiO_2 catalysts. Table 2 summarizes the changes in DHP conversion, THP production rate, 1-pentanol production rate, and THP selectivity with reaction temperatures (150, 180 and 200 °C) and Ni loading of catalyst (10 and 30 wt%). DHP conversion and THP production rate at 150 °C were negligible over SiO_2, indicating that any activity arises from the metallic Ni sites. Over $10\text{-}Ni/SiO_2$, the DHP conversion increased five times from 3.5% at 150 °C to 15.8% at 200 °C. The corresponding THP production rate more than doubled from 104.1 mmol h^{-1} $g_{cat}{}^{-1}$ at 150 °C to 263.5 mmol h^{-1} $g_{cat}{}^{-1}$ at 200 °C. The 1-pentanol production rate also increased from 0.01 mmol h^{-1} $g_{cat}{}^{-1}$ to 0.27 mmol h^{-1} $g_{cat}{}^{-1}$ with rise in temperature, but the selectivity to THP remained >99.8%. This indicates that THP is the kinetically favored product, in contrast to the previous thermodynamic calculations. Over $30\text{-}Ni/SiO_2$, DHP conversion increased from 80.2% at 150 °C to 98.0% at 200 °C, which is outside the kinetic regime. The highest rate of THP formation observed was 701 mmol h^{-1} $g_{cat}{}^{-1}$ over $30\text{-}Ni/SiO_2$ at 200 °C. Despite operating at near complete conversion over $30\text{-}Ni/SiO_2$, the 1-pentanol production rate remained <0.5 mmol h^{-1} and no other side products were observed by GC-MS. The conversion of DHP to THP was quantitative with >99.8% selectivity to THP over the range of temperatures and conversions studied, demonstrating that DHP hydrogenation over Ni/SiO_2 is a robust chemical pathway for production of high purity THP. The $10\text{-}Ni/SiO_2$ catalyst was used for all kinetic studies that follow. The apparent activation energy, E_a, of THP production over $10\text{-}Ni/SiO_2$ was 31.0 ± 0.1 kJ mol^{-1}, as seen from the Arrhenius plot in Fig. 4. The E_a of 1-pentanol production was 91.1 kJ mol^{-1}, which was three times higher than the E_a of THP formation. The kinetic results of THP production further show that the unwanted over-hydrogenolysis of THP to 1-pentanol can be minimized by operating at lower reaction temperatures.

Table 2 DHP conversion, product STY and selectivity as a function of reaction temperature. Reaction conditions: 150–200 °C, 200 psig, 0.1 g catalyst, 0.1 mL min^{-1} DHP, 100 mL min^{-1} H_2, 24 h

Catalyst	Reaction temperature (°C)	DHP conversion (%)	THP rate (mmol h^{-1} $g_{cat}{}^{-1}$)	1-Pentanol rate (mmol h^{-1} $g_{cat}{}^{-1}$)	THP selectivity (%)
SiO_2	150	0.05	0	0	N/A
$10\text{-}Ni/SiO_2$	150	3.5	104.1	0.01	99.98
$10\text{-}Ni/SiO_2$	180	9.5	191.3	0.19	99.89
$10\text{-}Ni/SiO_2$	200	15.8	263.5	0.27	99.89
$30\text{-}Ni/SiO_2$	150	80.2	618.1	0.43	99.94
$30\text{-}Ni/SiO_2$	180	89.3	689.4	0.48	99.93
$30\text{-}Ni/SiO_2$	200	98.0	701.0	0.49	99.93

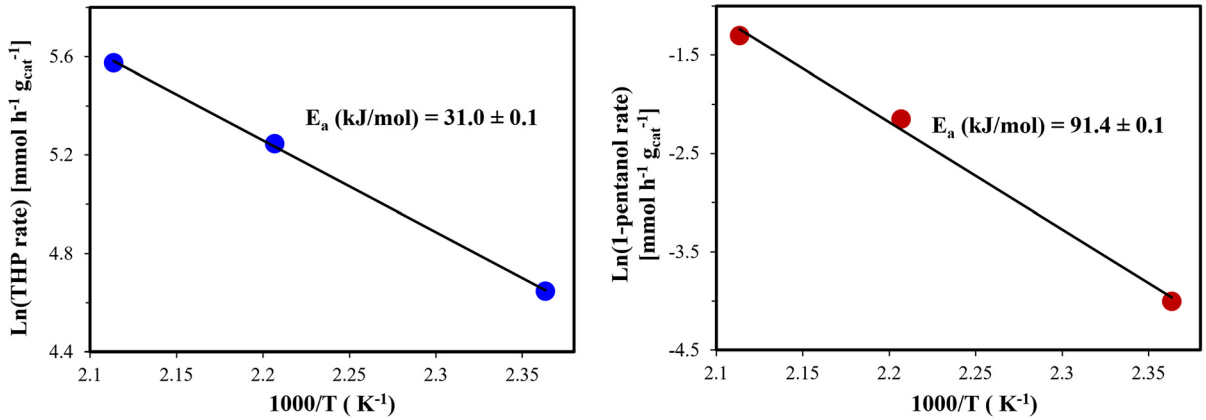

Fig. 4 Arrhenius plots of THP rate and 1-pentanol rate during DHP hydrogenation to THP, with apparent activation energies listed. Reaction conditions: 150–200 °C, 200 psig, 0.1 g 10-Ni/SiO_2, 0.1 mL min^{-1} DHP, 100 mL min^{-1} H_2, 24 h at each temperature, catalyst bed replaced when temperature varied.

3.2. Reaction orders of THP formation from partial pressure experiments

The reaction orders of DHP hydrogenation to THP with respect to the partial pressures of H_2, DHP, and THP are shown in the log–log plots of Fig. 5(A–C). As the H_2 artial pressure was varied from 100 to 250 psig, the THP rate increased from 14.1 to 34.3 mmol h^{-1} g_{cat}^{-1}. The corresponding reaction order with respect to H_2 partial pressure was 2nd order, the highest observed reaction order. As the DHP partial pressure was increased from 5 to 20 psig, the rate of THP formation increased from 35.2 to 158.4 mmol h^{-1}, corresponding to a reaction order of 1 with respect to DHP partial pressure. When THP was co-fed at a partial pressure of 0.5–3.5 psig, the rate of

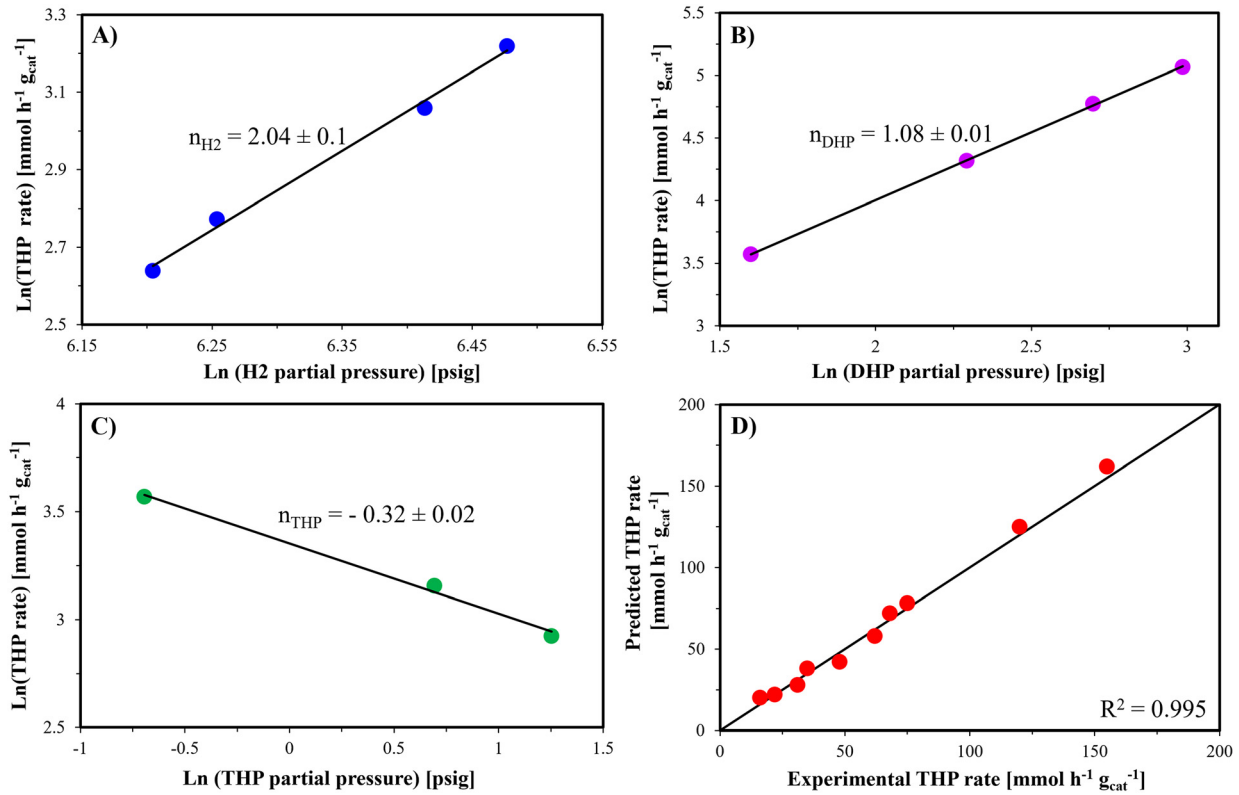

Fig. 5 Log–log plots of THP production rate as a function of: (A) H_2 partial pressure; (B) DHP partial pressure; and (C) THP partial pressure. (D) Parity plot of predicted THP rate *vs.* experimental THP rate based on the kinetic model in eqn (7). Reaction conditions: 150 °C, 200 psig, 0.1 g 10-Ni/SiO_2, 0.1 mL min^{-1} DHP, 100 mL min^{-1} H_2, 24 h at each condition.

THP formation decreased from 35.2 to 18.6 mmol h^{-1}. The corresponding reaction order of DHP hydrogenation was −0.3 with respect to THP partial pressure. The negative order dependence on THP partial pressure indicates the inhibitive effect of THP adsorption on catalyst activity.

3.3. Hougen–Watson kinetic model for DHP hydrogenation to THP

A kinetic model for DHP hydrogenation to THP was proposed using Hougen–Watson (HW) kinetics. The first step is the reversible adsorption of DHP onto the Ni/SiO_2 surface (eqn (3)), and the second step is the dissociative adsorption of H_2 (eqn (4)). This is followed by the surface reaction between adsorbed DHP and 2H to form THP (eqn (5)). The last step is the desorption of the product THP (eqn (6)). Vlachos *et al.* performed DFT calculations on the hydrogenation of dihydrofuran (DHF) to THF on Pd(111) catalysts and observed that the rate limiting step was the hydrogenation of DHF to trihydrofuran.[38] Similarly, experimental results for hydrogenation of DHP to THP in this work indicate the rate limiting step was likely the first hydrogenation of DHP to trihydropyran, the latter being an unobserved intermediate that rapidly hydrogenates to THP. The hydrogenation of DHP to trihydropyran and subsequent hydrogenation to THP have been considered as one step (eqn (5)), which is assumed to be the rate limiting step with rate constant k_3. All other steps (eqn (3), (4), and (6)) are assumed to be in quasi-equilibrium with equilibrium rate constants K_1, K_2 and K_4. The HW kinetic model and the corresponding equation for the least squares error are displayed in eqn (7) and (8) respectively. The fitted rate constants are shown in Table 3 and the parity plot of predicted rate *vs.* experimental rate is shown in Fig. 5D. In previous work, a Hougen–Watson kinetic model for DHP production from THFA dehydration has been demonstrated in a similar manner.[39]

$$\mathrm{DHP} + \theta \overset{K_1}{\longleftrightarrow} \mathrm{DHP_{ads}} \tag{3}$$

$$\mathrm{H_2} + 2\theta \overset{K_2}{\longleftrightarrow} 2\mathrm{H_{ads}} \tag{4}$$

$$\mathrm{DHP_{ads}} + 2\mathrm{H_{ads}} \overset{k_3}{\longrightarrow} \mathrm{THP_{ads}} + 2\theta \tag{5}$$

$$\mathrm{THP_{ads}} \overset{K_4}{\longleftrightarrow} \mathrm{THP} + \theta \tag{6}$$

$$r = \frac{k_3 K_1 P_{\mathrm{DHP}} \left(K_2 P_{\mathrm{H_2}}\right)^2}{1 + K_1 P_{\mathrm{DHP}} + \sqrt{K_2 P_{\mathrm{H_2}}} + \dfrac{P_{\mathrm{THP}}}{K_4}} \tag{7}$$

$$R^2 = 1 - \frac{\sum_{i=1}^{n} \left(r_{\mathrm{experimental}} - r_{\mathrm{model}}\right)^2}{\sum_{i=1}^{n} r_{\mathrm{experimental}}{}^2} \tag{8}$$

3.4. Ni/SiO_2 catalyst characterization and deactivation

The 10-Ni/SiO_2 catalyst was studied for 100 h time on stream (TOS), then regenerated with *in situ* calcination and reduction, and studied for another 30 h TOS. Fig. 6 shows the variation in THP rate with TOS for the fresh catalyst and regenerated catalyst. For the first 24 h, the rate of THP formation was nearly constant at 205 mmol h^{-1} $g_{cat}{}^{-1}$ at a DHP conversion of 12%. The THP rate then decreased monotonically and reached 75 mmol h^{-1} $g_{cat}{}^{-1}$ at 95 h TOS. The first-order deactivation rate constant for the catalyst was determined from the slope of the ln(THP rate) *vs.* TOS graph to be 0.012 h^{-1}. Fig. 7 shows the TGA curves for the fresh and spent catalyst (before and after the 100 h TOS run) from 0–600 °C in O_2 flow. The fresh catalyst had minimal loss in sample weight (<5 wt%) while the spent catalyst had a 50 wt% loss in mass of sample. TGA was also carried out in N_2 flow and both the fresh and spent catalyst had negligible loss in sample weight. Table 4 lists the catalyst characterization results of the fresh and spent 10-Ni/SiO_2 catalyst using N_2 physisorption, CO chemisorption and ICP-OES. The BET surface area of the catalyst decreased from 264 to 221 m^2 g^{-1}, indicating pore blocking of the catalyst. Ni dispersion also decreased from 18.6% to 12.5%, indicating

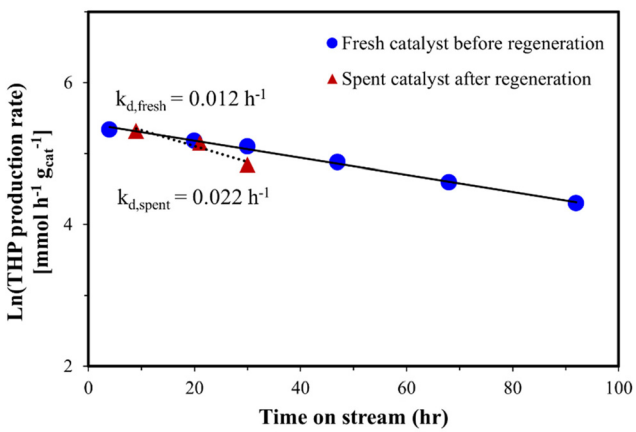

Fig. 6 Variation in THP formation rate with reaction time on stream (TOS). Reaction conditions: 150 °C, 200 psig, 0.1 g 10-Ni/SiO_2, 0.1 mL min^{-1} DHP, 100 mL min^{-1} H_2, 100 h. Catalyst regenerated *in situ* by calcination with 100 mL min^{-1} of 1% O_2/Ar at 400 °C followed by reduction with 100 mL min^{-1} H_2 at 500 °C, then reaction continued for another 30 h.

Table 3 Estimated kinetic parameters for DHP hydrogenation to THP over Ni/SiO_2 from the kinetic model shown in eqn (5)

Catalyst	K_1	K_2	k_3 [mmol h^{-1} $g_{cat}{}^{-1}$ $psig^{-3}$]	$1/K_4$
10-Ni/SiO_2	0.0127 ± 0.005	0.0225 ± 0.002	6.13 ± 0.3	0.11 ± 0.8

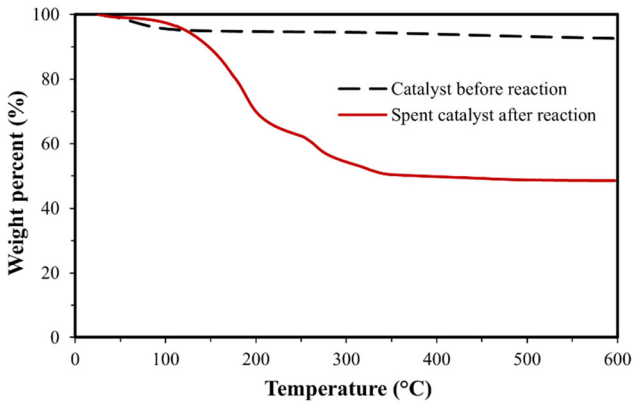

Fig. 7 Thermogravimetric analysis (TGA) of fresh and spent 10-Ni/SiO_2, *i.e.,* before and after 100 h TOS reaction. Experimental conditions: 20–600 °C at 10 °C min^{-1} in 50 mL min^{-1} O_2 flow.

Table 4 Characterization of fresh and spent 10-Ni/SiO_2 catalyst, *i.e.* before and after 100 h TOS reaction, using N_2 physisorption, CO chemisorption, and ICP-OES

Property	Fresh 10-Ni/SiO_2	Spent 10-Ni/SiO_2
BET surface area (m^2 g^{-1})	264	221
CO uptake (μmol g_{cat}^{-1})	85	76
Ni dispersion ($Ni_{surface}/Ni_{bulk}$)	18.6	12.5
Ni amount (wt%)	10.2	9.8

that Ni sites are sintering during the reaction. The Ni content of the catalyst did not change much, demonstrating that Ni leaching is not occurring. After regeneration by *in situ* calcination in 1% O_2/Ar at 400 °C and reduction in H_2 at 500 °C, the THP rate recovered to 200 mmol h^{-1} g_{cat}^{-1} (Fig. 6). After 30 h TOS with the regenerated catalyst, the THP rate had decreased to 125 mmol h^{-1} g_{cat}^{-1}. The deactivation rate constant for the regenerated catalyst is 1.8 times higher at 0.022 h^{-1}. The TOS study shows that the catalyst deactivates due to coke deposition, pore blocking, and Ni sintering, but can be regenerated to achieve THP formation rates nearly as high as those of the fresh catalyst.

3.5. Inertness of THP to polymerization

A critical property of solvents is their chemical stability at harsh reaction conditions. THF has a ring strain energy (RSE) of 6.9 kcal mol^{-1}, but THP has a much lower RSE of 2.0 kcal mol^{-1}.[40–42] Five-membered cyclic ethers such as THF and MeTHF are susceptible to ring-opening polymerization (ROP) to form polyethers as undesired side products, especially in the presence of acidic catalysts or reagents.[43] We hypothesized that six-membered THP would be more resistant to ROP due to its negligible ring strain. To demonstrate the superior chemical stability of THP as a solvent, we compared the polymerization behavior of THF and THP under identical conditions. Table 5 shows the differences in polymerization of THF and THP using different strongly acidic catalysts (BF_3·Et_2O and CF_3SO_3H), monomer/catalyst molar ratios (100/10 and 100/1), and temperatures (0, 23, and 80 °C). While THF polymerization was observed at all conditions tested, THP remained intact with 0% conversion at all conditions. With 10 mol% BF_3·Et_2O, 43% conversion of THF was achieved in 24 h to afford poly(THF), with M_n = 37.3 kg mol^{-1} and relatively narrow dispersity ($Đ$) = 1.17. A similar THF conversion of 45% was achieved with CF_3SO_3H, but the resulting poly(THF) has a much lower M_n = 1.6 kg mol^{-1} and broader $Đ$ = 1.58. When the catalyst loading was decreased to 1 mol%, BF_3·Et_2O achieved only 7% THF conversion after 24 h but CF_3SO_3H achieved 77% THF conversion after 24 h, affording poly(THF) with M_n = 24.8 kg mol^{-1} and $Đ$ = 1.13. Poly(THF) formation and lack of poly(THP) formation was verified using ^{1}H NMR (Fig. S2†). Poly(THF) was observed to be a semi-crystalline material with a melting-transition temperature (T_m) of 30 °C, as determined by DSC (Fig. S3†).

Table 5 Polymerization of THF and THP with varying catalysts, monomer to catalyst ratios, and temperatures[a]

Catalyst	[Monomer]/[Cat]	T (°C)	Conversion[b] (%) THF	THP
BF_3·Et_2O	100/10	0	43	0
CF_3SO_3H	100/10	0	45	0
BF_3·Et_2O	100/1	0	7	0
CF_3SO_3H	100/1	0	77	0
CF_3SO_3H	100/10	23	17	0
$Yb(OTf)_3$	100/1	80	—	0

[a] Conditions: polymerization was conducted in bulk monomer for 1 day with THF, and for 3 days with THP. [b] Monomer conversion was determined by ^{1}H NMR spectra.

The inability to polymerize THP under homopolymerization conditions demonstrated the inert nature of THP to ring opening. However, in some cases, a low ring strain monomer can be incorporated into polymer chains by copolymerization with a high ring strain comonomer.[44,45] Therefore, the copolymerization of THP (low ring strain) and THF (high ring strain) was further explored. The results are shown in Table 6, which indicated that only THF was selectively polymerized (Fig. S5†), while THP polymerization was still not observed. Specifically, 30% THF was converted to poly(THF) at 0 °C with [THF]/[THP]/[BF_3·Et_2O] = 100/100/10 after 3 days. The corresponding M_n and $Đ$ of the poly(THF) were 34.5 kg mol^{-1} and 1.16,

Table 6 Copolymerization of THF and THP with varying catalysts and temperatures[a]

Catalyst	[THF]/[THP]/[Cat]	T (°C)	Conversion[b] (%) THF	THP
BF_3·Et_2O	100/100/10	0	30	0
CF_3SO_3H	100/100/10	0	21	0
CF_3SO_3H	100/100/10	−30	13	0

[a] Conditions: polymerization was conducted in bulk monomer for 3 days. [b] Monomer conversion was determined by ^{1}H NMR spectra.

respectively. Similarly, THF conversion was 21% and 13% at 0 °C and −30 °C, respectively, with [THF]/[THP]/[CF_3SO_3H] = 100/100/10 after 3 days, but THP conversion was still 0%. The separated poly(THF) was confirmed by ^{1}H NMR (Fig. S2†) and characterized using DSC and TGA (Fig. S3†). These copolymerization results further confirmed the inertness of THP towards polymerization. Overall, the above extensive polymerization and copolymerization studies under various conditions demonstrated that THP is highly stable under conditions that THF is readily polymerized. This non-polymerizability, coupled with its biorenewability and higher boiling point, confirms our hypothesis of THP being a more stable solvent than THF or MeTHF.

3.6. Technoeconomic analysis of THP production

In previous work, we have shown that 1,5-PDO can be manufactured at a minimum selling price (MSP) of $1973 per ton when the furfural feedstock costs $1000 per ton and the 1,5-PDO production volume is 37 000 ton per year.[46] An extensive technoeconomic analysis of furfural production from lignocellulosic biomass fractionation has also been carried out in the past.[47] High purity DHP is produced as an intermediate during 1,5-PDO production at an MSP of $1478 per ton and production volume of 16 300 ton per year. Using these values, the minimum selling price (MSP) of THP produced from hydrogenation of DHP with 30-Ni/SiO_2 has been assessed. The process flow diagram is shown in Fig. 1, and Table S1† lists the corresponding temperature, pressure, and mass balance of each stream. The reaction data for the DHP production from THP was taken from the high conversion data (last entry in Table 2). Tables S2–4† summarize the economic parameters and assumptions for a commercial THP production unit, including plant operating hours, capital costs, variable operating costs, and fixed operating costs. Based on this analysis, THP can be produced at an MSP of $1812 per ton and production volume of 16 185 ton per year when the DHP feedstock price is $1478 per ton and feed rate is 16 300 ton per year. The corresponding purity of THP in the product stream is 97.8%. Fig. 8 shows the price of DHP feedstock is the main cost driver of the THP production process, constituting 81.5% of the total required cost.

We also conducted a sensitivity analysis for the THP production process as a function DHP feedstock price ($1000–3500 per ton) and plant production volume (3000–18 000 ton per year). With new technologies enabling cheaper production of furfural, the price of DHP is expected to drop below $1478 per ton. The results in Fig. 9 demonstrate that the MSP of THP is $1200–1400 per ton when the DHP feedstock costs $1000 per ton, enabling THP manufacturing to be competitive with the commercial market price of petroleum-derived THF ($900–1400 per ton). When the DHP feedstock price increases from $1000 per ton to $3500 per ton, the MSP of THP also rises from $1200 per ton to >$3000 per ton. On the other hand, the MSP of THP does not change much with the THP production volume for a given DHP feedstock price, decreasing by only $300–400 per ton when the THP production volume expands from 3000 ton per year to 80 000 ton per year. This demonstrates that THP is economically competitive with THF manufacturing when the price of DHP is <$1200 per ton over a wide range of production volumes.

3.7. Computational modeling of solvent properties of THP

A major challenge with commercialization of new biobased solvents like THP is the identification of potential applications. Using COSMO-RS to model the σ-profiles of THP and other industrially used solvents, we can determine which solvents are most similar to THP and then attempt to replace them with THP.[35] This approach measures similarity based on the chemical properties of solvents as opposed to their functional groups alone. We calculated the Euclidean distances between the THP and 1008 other solvents and defined a solvent's similarity score to be its distance to THP normalized by the average distance of all solvents to THP. The lower the score, the higher the similarity. Fig. 10 compares the σ-profiles of THP with THF and dichloromethane (DCM). THF and THP have highly similar σ-profiles, leading to a small Euclidean distance between these profiles and a similarity score of 0.25 for

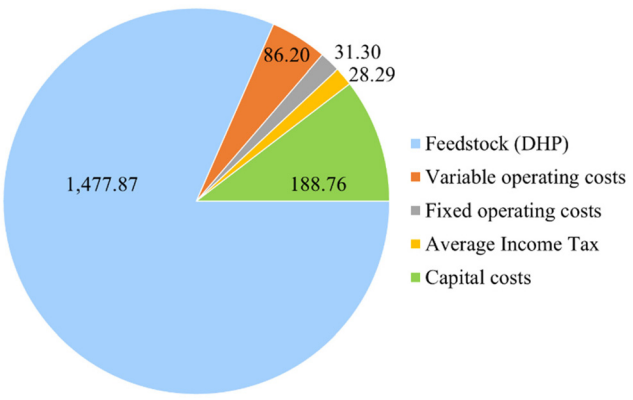

Fig. 8 Minimum selling price ($ per ton) breakdown for production of THP from hydrogenation of DHP over 30-Ni/SiO_2 in a packed bed reactor at a DHP feed rate of 16 300 ton per year.

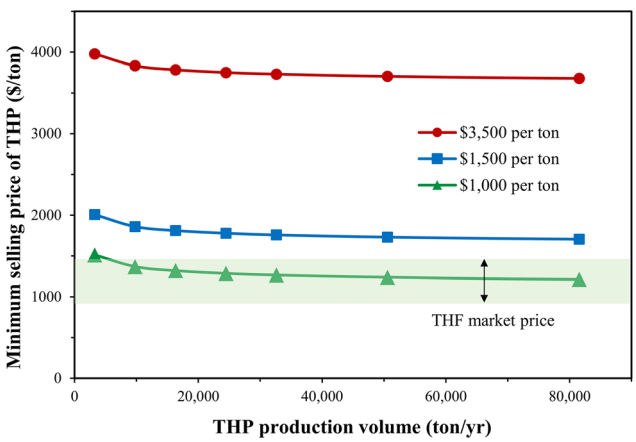

Fig. 9 Minimum selling price of THP as a function of THP production volume for three different DHP feedstock prices.

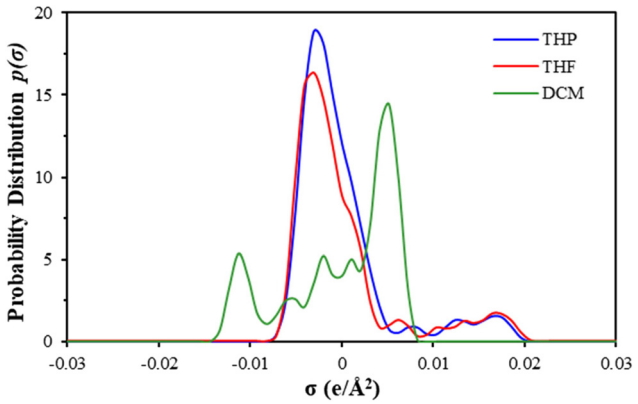

Fig. 10 σ-profiles of THP, THF, and dichloromethane (DCM) as predicted from COSMO-RS. The similarity rankings of THF and DCM corresponding to THP are 0.4% and 78.8%, respectively.

THF. On the other hand, DCM has a very different σ-profile with a high similarity score of 78.8, identifying it as a dissimilar solvent of THP.

Table 7 lists the 10 most similar solvents to THP and their corresponding similarity scores, with 2-methyltetrahydrofuran (MeTHF), diethyl ether, tetrahydropthiopyran, and THF in the top 4. We have also added 2,5-dimethyltetrahydrofuran[48] and 2,2,5,5-tetramethyltetrahydrofuran[10] to the list as they are homologous compounds of THF and can be biomass-derived. However, their chemical properties are not as similar to THP, as evidenced by their higher similarity scores. Likewise, 1,4-dioxane ($C_4H_8O_2$) may appear to have a similar structure to THP, but it has a similarity score of 22.78, imparting it with very different properties. Our results also demonstrate why quantitative tools like COSMO-RS are required to assess solvent similarity, since general chemical intuition based on structures, molecular sizes or elemental compositions can be incorrect. Computational modeling also enables us to predict the dissolution of various polymers in a given solvent, which is critical for paint formulations, drug delivery, membrane science, and plastic recycling. Table 7 lists the computationally predicted solubilities of 8 common polymers in THP and the solvents mentioned above. The polymers include: ethylene vinyl alcohol (EVOH), low density polyethylene (LDPE), polyethylene terephthalate (PET), polypropylene (PP), polystyrene (PS), polyvinyl chloride (PVC), and two polyamides (PA): nylon-6 and nylon-66. Note that the temperature at which the solubility is predicted is determined by the boiling point of the solvent. Based on the predicted solubilities, THP could serve as a good solvent (defined as solubility in excess of 3 g per 100 g solution) for LDPE, PP, PS and PVC, and as a poor solvent for EVOH, PET, nylon 6 and nylon 66. THP could serve as an alternative to other solvents, especially MeTHF, THF, dimethyl THF, and cyclopentyl methyl ether, which have similar predicted solubilities for almost all polymers listed. These values could be used as input parameters in process modeling and techno-economic analyses to study the costs and benefits of using THP as an alternative solvent.

3.8. Applications of THP for upcycling of mixed plastics

We recently developed a solvent-targeted recovery and precipitation (STRAP) process to recycle components from multilayer plastic films.[49] The STRAP process selectively dissolves constituent polymers through a series of solvent washes, each designed to dissolve only a single polymer component. The solubility data in Table 7 indicate that THP has potential application as a selective solvent for STRAP processes of many plastic materials. For example, it could be used to selectively dissolve PP from PP/EVOH/PA mixture, which is the composition of an Amcor packaging film;[50] dissolve PS from PS/PET, an UltiDent sealing film;[51] or PVC from PVC/EVOH, a Desu plastic sheet.[52] These proposed applications are based on commercial products and demonstrate the applicability of THP to possible recycling processes. THP could also be used to

Table 7 Solubility predictions of 8 polymers in THP, the top 10 solvents most similar to THP, and two homologous compounds of THF. The similarity scores and boiling points of the solvents have also been listed

			Polymer solubility predictions (g polymer per 100 g solution)							
Solvent	Similarity score[a]	T^b (°C)	EVOH	LDPE	PET	PP	PS	PVC	Nylon-6	Nylon-66
THP	0.00	87.0	1.1	7.3	0.8	20.9	33.7	17.9	0.7	0.3
2-Methyl tetrahydrofuran	0.14	77.0	0.5	3.9	0.4	15.1	28.1	14.6	0.4	0.2
Diethyl ether	0.21	33.5	0.0	0.2	0.0	4.4	10.8	4.0	0.0	0.0
Tetrahydrothiopyran	0.24	120.0	1.3	39.8	5.4	40.3	46.7	26.0	2.5	0.8
Tetrahydrofuran	0.25	64.0	0.9	1.7	0.8	10.1	31.3	19.1	0.4	0.2
Pyrrolidine	0.27	85.5	19.2	5.7	2.8	15.0	32.2	22.4	2.1	1.2
Dimethyl ethanolamine	0.27	120.0	17.9	38.5	7.6	37.7	50.3	34.8	6.0	2.9
Methyl ethyl ether	0.28	6.4	0.0	0.0	0.0	1.3	9.4	4.2	0.0	0.0
1-Butanol	0.28	116.7	10.1	18.4	0.4	12.4	9.2	10.2	5.4	2.4
Cycloheptanone	0.28	120.0	8.3	30.1	3.9	27.2	41.7	27.9	3.2	1.4
Cyclopentyl methyl ether	0.29	105.0	0.9	19.6	0.6	31.3	33.6	14.6	0.8	0.3
2,5-Dimethyl tetrahydrofuran[c]	0.33	89.0	0.6	7.7	0.3	20.0	26.1	12.3	0.4	0.1
2,2,5,5-Tetramethyl tetrahydrofuran[c]	0.67	111.0	1.6	22.3	0.4	29.1	26.2	12.1	0.7	0.2

[a] Similarity score calculated from normalized Euclidean distance between solvent and THP from COSMO-RS. [b] Temperature of simulation is ~1 °C lower than boiling point of solvent. [c] Homologous compounds of THF.

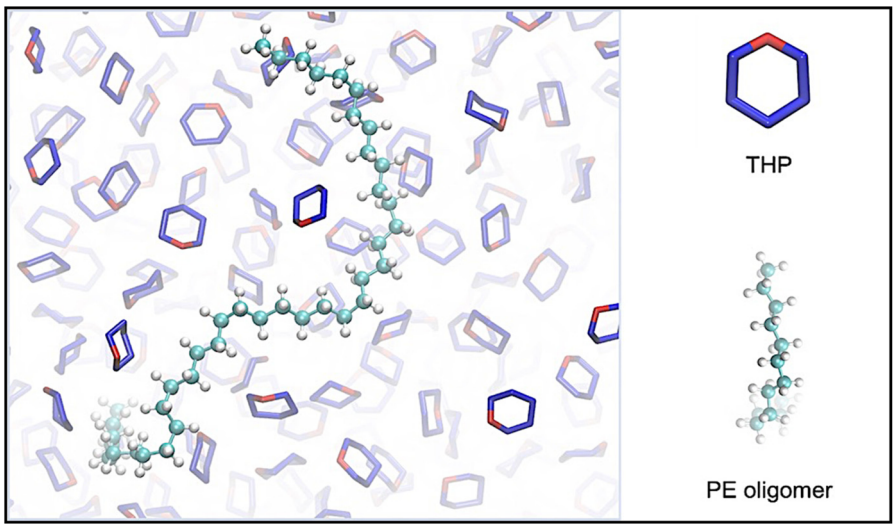

Fig. 11 MD simulation of an LDPE oligomer in solution of THP.

replace hazardous solvents in existing STRAP processes. For example, we recently reported a STRAP process in which toluene is used as a selective solvent to dissolve LDPE from a LDPE/EVOH/PET mixture.[53] The predicted solubilities in Table 7 indicate that THP should also dissolve LDPE but not EVOH or PET, and thus could be an alternative selective solvent to toluene. We performed MD simulations to further support the prediction that THP is a good solvent for an LDPE oligomer ($C_{40}H_{82}$), as shown in Fig. 11. We also calculated the radius of gyration (R_g) and the solvent accessible surface area (SASA) of the oligomer molecule from the MD trajectories to evaluate the tendency of the oligomer to collapse into a folded conformation (indicative of poor solvent behavior) or extend into an elongated conformation (indicative of good solvent behavior).[54,55] Fig. S4† shows the oligomer's R_g-SASA distributions in THP and water. The oligomer molecule in water mostly obtains small values of R_g and SASA, indicating a preference for folded conformations. In THP, however, the oligomer tends to have large R_g and SASA, indicating elongated conformations. Since water is a poor solvent for LDPE, the different behavior of the oligomer chain in THP indicates that it is a good solvent in agreement with COSMO-RS predictions.

4. Conclusions

Tetrahydropyran (THP) is a green solvent that does not form peroxides, offers excellent solvent properties, and is an economically competitive replacement for tetrahydrofuran (THF). In this work, we have demonstrated a new pathway to produce biobased THP from hydrogenation of furfural-derived 3,4-dihydropyran (DHP) over Ni/SiO_2 catalysts in a packed bed reactor. The selectivity to THP was >99.8% at a carbon balance of ~100% over a wide range of DHP conversions and temperatures with 1-pentanol as the only detected side product. Kinetic experiments with 10-Ni/SiO_2 show that the apparent activation energy of THP and 1-pentanol formation is 31 kJ mol^{-1} and 91 kJ mol^{-1}, respectively, indicating that THP is the kinetically favored product. THP formation has been observed to be 2^{nd} order with respect to H_2 partial pressure and 1^{st} order with respect to DHP partial pressure. Addition of a THP co-feed is inhibitive to THP formation, leading to a −0.3 reaction order with respect to THP partial pressure. A rate law expression for THP formation has been determined using Hougen–Watson kinetics. A time on stream study was performed to quantify a first-order deactivation rate constant of 0.012 h^{-1} for 10-Ni/SiO_2 over 100 h. TGA analysis on the fresh and spent catalyst in O_2 flow showed a 50 wt% loss in sample weight of the spent catalyst, indicating that coke formation is a major factor in catalyst deactivation. THP was shown to have beneficial solvent properties including resistance to ring opening polymerization over a variety of catalysts and conditions that caused THF to polymerize. A techno-economic analysis determined that the MSP of THP can be competitive with the THF market price ($900–1400 per ton) at a DHP feedstock cost of $1000 per ton and a DHP feed rate of 16 300 ton per year. Lastly, COSMO-RS and MD simulations were used to model the solvent properties of THP, compare it to 1007 other solvents, and predict the solubilities of 8 common plastics. THP can be used to replace THF, MeTHF, dimethyl THF, and cyclopentyl methyl ether as the solvent to dissolve LDPE, PP, PS and PVC, and can be used for upcycling multilayer waste plastics through selective dissolution.

Author contributions

Investigation, formal analysis, and writing (original draft): RGD, MSK, PZ, ZL, CX. Writing (reviewing and editing), supervision, and funding acquisition: KJB, DJM, EXC, RCV and GWH. The final manuscript has been read and approved by all authors.

Conflicts of interest

The authors declare the following competing financial interest (s): GWH, KJB, and DJM have a financial interest in Pyran which is commercializing the technology to produce biomass-based C_5 chemicals from furfural.

Acknowledgements

This work was supported by the University of Wisconsin–Madison, Discovery to Product (D2P) with funding from the State of Wisconsin, and by the U.S. Department of Energy, Office of Energy Efficiency and Renewable Energy, Advanced Manufacturing Office (AMO) and Bioenergy Technologies Office (BETO) under Award Number DE-EE0009285. The work done at Colorado State University was performed as part of the BOTTLE™ Consortium and funded under contract no. DE-AC36-08GO28308 with the National Renewable Energy Laboratory, operated by Alliance for Sustainable Energy.

References

1 P. T. Anastas and J. B. Zimmerman, *Peer reviewed: design through the 12 principles of green engineering*, ACS Publications, 2003.
2 J. Sherwood, A. Constantinou, L. Moity, C. R. McElroy, T. J. Farmer, T. Duncan, W. Raverty, A. J. Hunt and J. H. Clark, Dihydrolevoglucosenone (Cyrene) as a bio-based alternative for dipolar aprotic solvents, *Chem. Commun.*, 2014, **50**(68), 9650–9652.
3 Solvents Market Size, Share & COVID-19 Impact Analysis, by Product Type (Alcohols, Ketones, Esters, and Others), Application (Paints & Coatings, Printing Inks, Industrial Cleaning, Adhesives, and Others), and Regional Forecast, 2021–2028. **https://www.fortunebusinessinsights.com/industrial-solvents-market-102135**.
4 D. M. Kochepka, L. P. Dill, D. Fockink and R. M. Lukasik, Contribution to the production and use of biomass-derived solvents: a review, *Acta Innov.*, 2020, **35**, 29–56.
5 D. F. Aycock, Solvent applications of 2-methyltetrahydrofuran in organometallic and biphasic reactions, *Org. Process Res. Dev.*, 2007, **11**(1), 156–159.
6 A. McMichael, Carcinogenicity of benzene, toluene and xylene: epidemiological and experimental evidence, *IARC Sci. Publ.*, 1988, 3–18.
7 B. Nelson, W. S. Brightwell, J. V. Setzer and T. L. O'Donohue, Reproductive toxicity of the industrial solvent 2-ethoxyethanol in rats and interactive effects of ethanol, *Environ. Health Perspect.*, 1984, **57**, 255–259.
8 C. M. Filley, W. Halliday and B. Kleinschmidt-DeMasters, The effects of toluene on the central nervous system, *J. Neuropathol. Exp. Neurol.*, 2004, **63**(1), 1–12.
9 V. Pace, P. Hoyos, L. Castoldi, D. de María, P. Alcántara and A. R, 2−Methyltetrahydrofuran (2−MeTHF): a biomass–derived solvent with broad application in organic chemistry, *ChemSusChem*, 2012, **5**(8), 1369–1379.
10 F. Byrne, B. Forier, G. Bossaert, C. Hoebers, T. J. Farmer, J. H. Clark and A. J. Hunt, 2, 2, 5, 5-Tetramethyltetrahydrofuran (TMTHF): a non-polar, non-peroxide forming ether replacement for hazardous hydrocarbon solvents, *Green Chem.*, 2017, **19**(15), 3671–3678.
11 Tetrahydropyran. **https://go.drugbank.com/drugs/DB02412** (accessed 01/19).
12 M. J. Zenker, R. C. Borden and M. A. Barlaz, Mineralization of 1, 4-dioxane in the presence of a structural analog, *Biodegradation*, 2000, **11**(4), 239–246.
13 H. Yasuda, Y. Uenoyama, O. Nobuta, S. Kobayashi and I. Ryu, Radical chain reactions using THP as a solvent, *Tetrahedron Lett.*, 2008, **49**(2), 367–370.
14 J. Howard and K. Ingold, Absolute rate constants for hydrocarbon autoxidation. XVIII. Oxidation of some acyclic ethers, *Can. J. Chem.*, 1970, **48**(6), 873–880.
15 H. Matsubara, S. Suzuki and S. Hirano, An ab initio and DFT study of the autoxidation of THF and THP, *Org. Biomol. Chem.*, 2015, **13**(16), 4686–4692.
16 F. Dainton, K. Ivin and R. LaFlair, Kinetics of anionic polymerization of styrene in tetrahydropyran, *Eur. Polym. J.*, 1969, **5**(3), 379–386.
17 F. Dainton, K. Hui and K. Ivin, Kinetics of anionic polymerization of α-methylstyrene in tetrahydropyran, *Eur. Polym. J.*, 1969, **5**(3), 387–394.
18 X. Wang, E. Yasukawa and S. Mori, Electrochemical behavior of lithium imide/cyclic ether electrolytes for 4 V lithium metal rechargeable batteries, *J. Electrochem. Soc.*, 1999, **146**(11), 3992.
19 S. Kobayashi, T. Tamura, S. Yoshimoto, T. Kawakami and A. Masuyama, 4−Methyltetrahydropyran (4−MeTHP): Application as an Organic Reaction Solvent, *Chem. - Asian J.*, 2019, **14**(21), 3921–3937.
20 M. Stekrova, P. Mäki-Arvela, N. Kumar, E. Behravesh, A. Aho, Q. Balme, K. P. Volcho, N. F. Salakhutdinov and D. Y. Murzin, Prins cyclization: Synthesis of compounds with tetrahydropyran moiety over heterogeneous catalysts, *J. Mol. Catal. A: Chem.*, 2015, **410**, 260–270.
21 S. Di Tommaso, P. Rotureau, B. Sirjean, R. Fournet, W. Benaissa, P. Gruez and C. Adamo, A mechanistic and experimental study on the diethyl ether oxidation, *Process Saf. Prog.*, 2014, **33**(1), 64–69.
22 A. Yamaguchi, N. Hiyoshi, O. Sato, K. K. Bando and M. Shirai, Enhancement of cyclic ether formation from polyalcohol compounds in high temperature liquid water by high pressure carbon dioxide, *Green Chem.*, 2009, **11**(1), 48–52.
23 L. Zheng, D. J. McClelland, K. M. Rehmann, K. J. Barnett, G. W. Huber and J. Klier, Bio-based 1, 5-Pentanediol as a Replacement for Petroleum-Derived 1, 6-Hexanediol for Polyester Polyols, Coatings, and Adhesives, *ACS Sustainable Chem. Eng.*, 2022, **10**(18), 5781–5791.
24 V. Kumar, P. Binod, R. Sindhu, E. Gnansounou and V. Ahluwalia, Bioconversion of pentose sugars to value

added chemicals and fuels: Recent trends, challenges and possibilities, *Bioresour. Technol.*, 2018, **269**, 443–451.

25 Furfural Market by Raw Material (Sugarcane Bagasse, Corncob, Rice Husk and Others), Application (Derivatives (Furfural Alcohol and Other Derivatives), solvent) and Region (Asia-Pacific, Americas, Europe,Middle East and Africa) – Global Forecast to 2024. **https://www.marketsandmarkets.com/Market-Reports/furfural-market-101056456.html**.

26 K. Yan, G. Wu, T. Lafleur and C. Jarvis, Production, properties and catalytic hydrogenation of furfural to fuel additives and value-added chemicals, *Renewable Sustainable Energy Rev.*, 2014, **38**, 663–676.

27 G. W. Huber, J. A. Dumesic, K. J. Barnett and Z. J. Brentzel. *Production of 1, 5-pentanediol via upgrading of tetrahydrofufuryl alcohol*. 2019.

28 K. J. Barnett, D. J. McClelland and G. W. Huber, Autocatalytic hydration of Dihydropyran to 1, 5-Pentanediol precursors via in situ formation of liquid-and solid-phase acids, *ACS Sustainable Chem. Eng.*, 2017, **5**(11), 10223–10230.

29 Z. J. Brentzel, K. J. Barnett, K. Huang, C. T. Maravelias, J. A. Dumesic and G. W. Huber, Chemicals from biomass: Combining ring–opening tautomerization and hydrogenation reactions to produce 1, 5—pentanediol from furfural, *ChemSusChem*, 2017, **10**(7), 1351–1355.

30 A. Klamt and G. Schüürmann, COSMO: a new approach to dielectric screening in solvents with explicit expressions for the screening energy and its gradient, *J. Chem. Soc., Perkin Trans. 2*, 1993, 799–805.

31 A. Klamt, Conductor-like screening model for real solvents: a new approach to the quantitative calculation of solvation phenomena, *J. Phys. Chem.*, 1995, **99**(7), 2224–2235.

32 COSMOlogic GmbH & Co KG, COSMOtherm Reference Manual Release 19. 2019.

33 F. Eckert and A. Klamt, Fast solvent screening via quantum chemistry: COSMO–RS approach, *AlChE J.*, 2002, **48**(2), 369–385.

34 A. Klamt, F. Eckert, M. Hornig, M. E. Beck and T. Bürger, Prediction of aqueous solubility of drugs and pesticides with COSMO–RS, *J. Comput. Chem.*, 2002, **23**(2), 275–281.

35 P. Zhou, K. L. Sánchez–Rivera, G. W. Huber and R. C. Van Lehn, Computational Approach for Rapidly Predicting Temperature–Dependent Polymer Solubilities Using Molecular–Scale Models, *ChemSusChem*, 2021, **14**(19), 4307–4316.

36 P. Zhou, J. Yu, K. L. Sánchez–Rivera, G. W. Huber and R. C. Van Lehn. Unpublished material.

37 V. Kuplenieks, D. Kreile, V. Slavinskaya and A. Avots, Hydrogenation of 2, 3-dihydropyran to tetrahydropyran, *Chem. Heterocycl. Compd.*, 1982, **18**(4), 351–354.

38 S. Wang, V. Vorotnikov and D. G. Vlachos, A DFT study of furan hydrogenation and ring opening on Pd (111), *Green Chem.*, 2014, **16**(2), 736–747.

39 L. Li, K. J. Barnett, D. J. McClelland, D. Zhao, G. Liu and G. W. Huber, Gas-phase dehydration of tetrahydrofurfuryl alcohol to dihydropyran over γ-Al2O3, *Appl. Catal., B*, 2019, **245**, 62–70.

40 R. Talukdar, Synthetically important ring opening reactions by alkoxybenzenes and alkoxynaphthalenes, *RSC Adv.*, 2020, **10**(52), 31363–31376.

41 K. B. Wiberg, The concept of strain in organic chemistry, *Angew. Chem., Int. Ed. Engl.*, 1986, **25**(4), 312–322.

42 M. P. Confer, T. Qu, P. A. Rupar and D. A. Dixon, Composite Correlated Molecular Orbital Theory Calculations of Ring Strain for Use in Predicting Polymerization Reactions, *ChemPhysChem*, 2022, e202200133.

43 R. Hoogenboom, Polyethers and polyoxazolines, in *Handbook of ring-opening polymerization*, 2009, pp. 141–164.

44 M. Hong and E. Y.-X. Chen, Coordination ring-opening copolymerization of naturally renewable α-methylene-γ-butyrolactone into unsaturated polyesters, *Macromolecules*, 2014, **47**(11), 3614–3624.

45 B. M. Stadler, S. Tin, A. Kux, R. Grauke, C. Koy, T. D. Tiemersma-Wegman, S. Hinze, H. Beck, M. O. Glocker and A. Brandt, Co-Oligomers of Renewable and "Inert" 2-MeTHF and Propylene Oxide for Use in Bio-Based Adhesives, *ACS Sustainable Chem. Eng.*, 2020, **8**(35), 13467–13480.

46 K. Huang, Z. J. Brentzel, K. J. Barnett, J. A. Dumesic, G. W. Huber and C. T. Maravelias, Conversion of furfural to 1, 5-pentanediol: Process synthesis and analysis, *ACS Sustainable Chem. Eng.*, 2017, **5**(6), 4699–4706.

47 K. Huang, W. Won, K. J. Barnett, Z. J. Brentzel, D. M. Alonso, G. W. Huber, J. A. Dumesic and C. T. Maravelias, Improving economics of lignocellulosic biofuels: An integrated strategy for coproducing 1, 5-pentanediol and ethanol, *Appl. Energy*, 2018, **213**, 585–594.

48 C. Zhang, Y. Wang, W. Yang and J. Zheng, Biobased 2, 5-Dimethyltetrahydrofuran as a Green Aprotic Ether Solvent, *Org. Process Res. Dev.*, 2022, **26**(9), 2685–2693.

49 T. W. Walker, N. Frelka, Z. Shen, A. K. Chew, J. Banick, S. Grey, M. S. Kim, J. A. Dumesic, V. Lehn, R. C. Huber and G. W, Recycling of multilayer plastic packaging materials by solvent-targeted recovery and precipitation, *Sci. Adv.*, 2020, **6**(47), eaba7599.

50 Amcor Duplex PP EVOH laminates for steam sterilization. **https://www.amcor.com/product-listing/duplex-pppp-pa-evoh-pa-pp** (accessed April 14).

51 UltiDent Scientific PLATESEAL™ ELISA FILM. **https://www.ultident.com/index.php/products/pcr/pcr-sealing/platesealtm-elisa-film.html** (accessed April 14).

52 Desu Tech PVC-EVOH-PVC. **https://desuplastic.com/evoh-plastic-sheet/pvc-evoh-pvc/**(accessed April 14).

53 K. L. Sánchez-Rivera, P. Zhou, M. S. Kim, L. D. González Chávez, S. Grey, K. Nelson, S.-C. Wang, I. Hermans, V. M. Zavala, R. C. Van Lehn and G. W. Huber, Reducing Antisolvent Use in the STRAP Process by Enabling a Temperature-Controlled Polymer Dissolution and Precipitation for the Recycling of Multilayer Plastic Films, *ChemSusChem*, 2021, **14**(19), 4317–4329.

54 P. d. De Gennes, Collapse of a polymer chain in poor solvents, *J. Phys., Lett.*, 1975, **36**(3), 55–57.

55 M. Rubinstein and R. H. Colby, *Polymer physics*, Oxford university press, New York, 2003, vol. 23.